Follow us @BoneJointRes

Freely available online OPEN ACCESS

BJR

CARTILAGE

Upregulated ribosome pathway plays a key role in HDAC4, improving the survival rate and biofunction of chondrocytes

L. Guo,
H. Guo,
Y. Zhang,
Z. Chen,
J. Sun,
G. Wu,
Y. Wang,
Y. Zhang,
X. Wei,
P. Li

From Second Hospital of Shanxi Medical University, Taiyuan, China

Aims

To explore the novel molecular mechanisms of histone deacetylase 4 (HDAC4) in chondrocytes via RNA sequencing (RNA-seq) analysis.

Methods

Empty adenovirus (EP) and a *HDAC4* overexpression adenovirus were transfected into cultured human chondrocytes. The cell survival rate was examined by real-time cell analysis (RTCA) and EdU and flow cytometry assays. Cell biofunction was detected by Western blotting. The expression profiles of messenger RNAs (mRNAs) in the EP and *HDAC4* transfection groups were assessed using whole-transcriptome sequencing (RNA-seq). Volcano plot, Gene Ontology, and pathway analyses were performed to identify differentially expressed genes (DEGs). For verification of the results, the A289E/S246/467/632 A sites of *HDAC4* were mutated to enhance the function of HDAC4 by increasing HDAC4 expression in the nucleus. RNA-seq was performed to identify the molecular mechanism of HDAC4 in chondrocytes. Finally, the top ten DEGs associated with ribosomes were verified by quantitative polymerase chain reaction (QPCR) in chondrocytes, and the top gene was verified both in vitro and in vivo.

Results

HDAC4 markedly improved the survival rate and biofunction of chondrocytes. RNA-seq analysis of the EP and *HDAC4* groups showed that HDAC4 induced 2,668 significant gene expression changes in chondrocytes (1,483 genes upregulated and 1,185 genes downregulated, $p < 0.05$), and ribosomes exhibited especially large increases. The results were confirmed by RNA-seq of the EP versus mutated *HDAC4* groups and the validations in vitro and in vivo.

Conclusion

The enhanced ribosome pathway plays a key role in the mechanism by which HDAC4 improves the survival rate and biofunction of chondrocytes.

Cite this article: *Bone Joint Res* 2023;12(7):433–446.

Keywords: Histone deacetylase 4, RNA sequencing, Ribosome, Chondrocyte, Gene mutation

Article focus

- The aim of this study was to reveal the novel molecular mechanisms by which histone deacetylase 4 (HDAC4) improves chondrocyte survival rate and biological function via mutagenesis analysis and RNA sequencing (RNA-seq).

Key messages

- HDAC4 markedly improves the survival rate and biofunction of chondrocytes.
- HDAC4 improves the survival rate and biofunction of chondrocytes by enhancing ribosome pathways.
- Supporting this conclusion, mutating the caspase cleavage site (A289) and 14-3-3 protein interaction sites (S246/467/632) increases the expression of HDAC4 in the nucleus.

Correspondence should be sent to Pengcui Li; email: lpc1977@163.com

doi: 10.1302/2046-3758.127.BJR-2022-0279.R2

Bone Joint Res 2023;12(7):433–446.

Strengths and limitations

- In this study, the A289E/S246/467/632 A sites of *HDAC4* were mutated to amplify the function of HDAC4 by increasing the expression of HDAC4 in the nucleus, and RNA-seq was performed to further discover the molecular mechanism of HDAC4 in chondrocytes.
- The functions of the selected genes should be further validated.

Introduction

Cartilage is a specialized connective tissue. Its main functions are to disperse and transfer load between joints, reduce friction, and help joints to move smoothly and painlessly. Chondrocytes are the only resident cell type in cartilage tissue and play a key role in maintaining the normal biological function of cartilage by secreting the major extracellular matrix (ECM).[1] Once chondrocyte dedifferentiation or death occurs, it will lead to progressive degeneration of cartilage, ultimately progressing to osteoarthritis (OA).[2,3] Thus, improving the survival rate and biofunction of chondrocytes is very important to protect cartilage from OA.

Histone deacetylase 4 (HDAC4) is the best characterized member of the HDAC class IIa family. This molecule is closely associated with cell proliferation, hypertrophy, apoptosis, and other processes during development and disease.[4] In cartilage tissues, mice lacking *HDAC4* die early during the postnatal period,[5] which indicates that HDAC4 plays an essential role in regulating cartilage and bone development. Studies have shown that HDAC4 represses chondrocyte hypertrophy and endochondral bone formation by inhibiting the function of myocyte-specific enhancer factor 2C (MEF2C) and runt-related transcription factor 2 (RUNX2).[6-8] A 2014 study showed that decreased HDAC4 contributes to chondrocyte hypertrophy and cartilage degeneration, which in turn accelerates the pathogenesis of OA cartilage degeneration.[9] These results suggest that repressing chondrocyte hypertrophy might be the main molecular mechanism by which HDAC4 functions in cartilage development and OA progression. However, an earlier study on HDAC4 by Guan et al[10] discovered that the subcellular location of HDAC4 might be associated with chondrocyte proliferation in growth plates. Gao et al[11] found that HDAC4 expression in chondrocytes contributes to angiogenesis in the growth plate, and its absence in vivo negatively affects growth plates. Therefore, in addition to chondrocyte hypertrophy, HDAC4 may also modulate other biological functions of chondrocytes. However, the regulatory mechanism is still unclear. In this study, we used RNA sequencing (RNA-seq) to explore the novel molecular mechanisms of HDAC4 in chondrocytes.

Methods

A number of the methods reported in this article were also previously reported in Guo et al.[12]

Chondrocyte isolation and primary culture. Cartilage slices were removed from 'relatively normal' cartilage samples of the tibia obtained during total knee arthroplasty and washed in Dulbecco's modified Eagle's medium (DMEM) (Invitrogen; Thermo Fisher Scientific, USA). Chondrocytes were isolated as previously described.[13] Primary chondrocytes were incubated in DMEM containing 10% fetal bovine serum (FBS), L-glutamine (Invitrogen), and antibiotics (penicillin and streptomycin) (MilliporeSigma, USA) at 37°C in 5% CO_2 and allowed to attach to the surface of culture dishes (Nalge Nunc International Corp, USA). After 48 hours, immunocytochemistry analysis of the chondrocyte phenotype was performed as described previously using anti-type I collagen (ab34710; Abcam, USA) and anti-type II collagen monoclonal antibodies (ab34712; Abcam, USA).[14] The cells were positive for type II collagen and negative for type I collagen (Figure 1a).

Overexpressing HDAC4 in chondrocytes. HDAC4 adenovirus and mutated HDAC4 adenovirus, the caspase-2/3 cleaved site (Asp-289), and 14-3-3 binding sites (Ser-246, Ser-467, and Ser-632) were mutated and constructed by GeneChem (China). Human chondrocytes were plated at 50% to 60% confluence, and after 24 hours the cells were transfected at a confluence of 70% to 90% (60 mm dish: 1×10^6). Adenovirus DNA (1×10^6 plaque-forming units (PFUs)/ml) was prepared and added to the cells. Then 12 hours after transfection, the cells were cultured in 10% FBS medium at 37°C; 48 hours after transfection, the transfection rates were detected by fluorescence imaging (Olympus, Japan) and flow cytometry (CyFlow Cube 6; Partec, Germany). The mean transfection rates were as follows: empty adenovirus (EP) control: 85.6% (standard deviation (SD 4.7%); HDAC4: 90.52 (SD 5.7%) (Figures 1b and 1c), mutated HDAC4: 91.9 (SD 3.9%) (Supplementary Figure aa). Then 70 hours after transfection, the biomarkers of chondrocyte differentiation RUNX2, type X collagen (Col-X), and matrix metallopeptidase-13 (MMP-13) were detected by Western blotting.

Real-time cell analysis. FBS medium (10%, 100 µl) containing 2×10^3 to 4×10^3 cells was loaded in each well of a 96-well plate (ACEA Biosciences, Agilent Technologies, USA). The plate was incubated for a minimum of 30 minutes in a humidified (37°C) 5% CO_2 incubator and then inserted into a real-time cell electronic sensing system (ACEA Biosciences); the cell survival rate was monitored for 70 hours.

Cell viability measurement by flow cytometry. The viability of cells was detected by phycoerythrin (PE) Annexin V and 7-amino-actinomycin (7-AAD) staining kits (BD Biosciences, USA). In the kits, cells that are considered viable are PE Annexin V and 7-AAD negative; cells that are in early apoptosis are PE Annexin V positive and 7-AAD negative; and cells that are in late apoptosis or already dead are both PE Annexin V and 7-AAD positive. We tested according to the manufacturer's instructions. The percentages of live and dead cells were quantified by fluorescence-activated cell sorting analysis on a MACSQuant instrument (Miltenyi Biotec, Germany). The experiment was repeated three times.

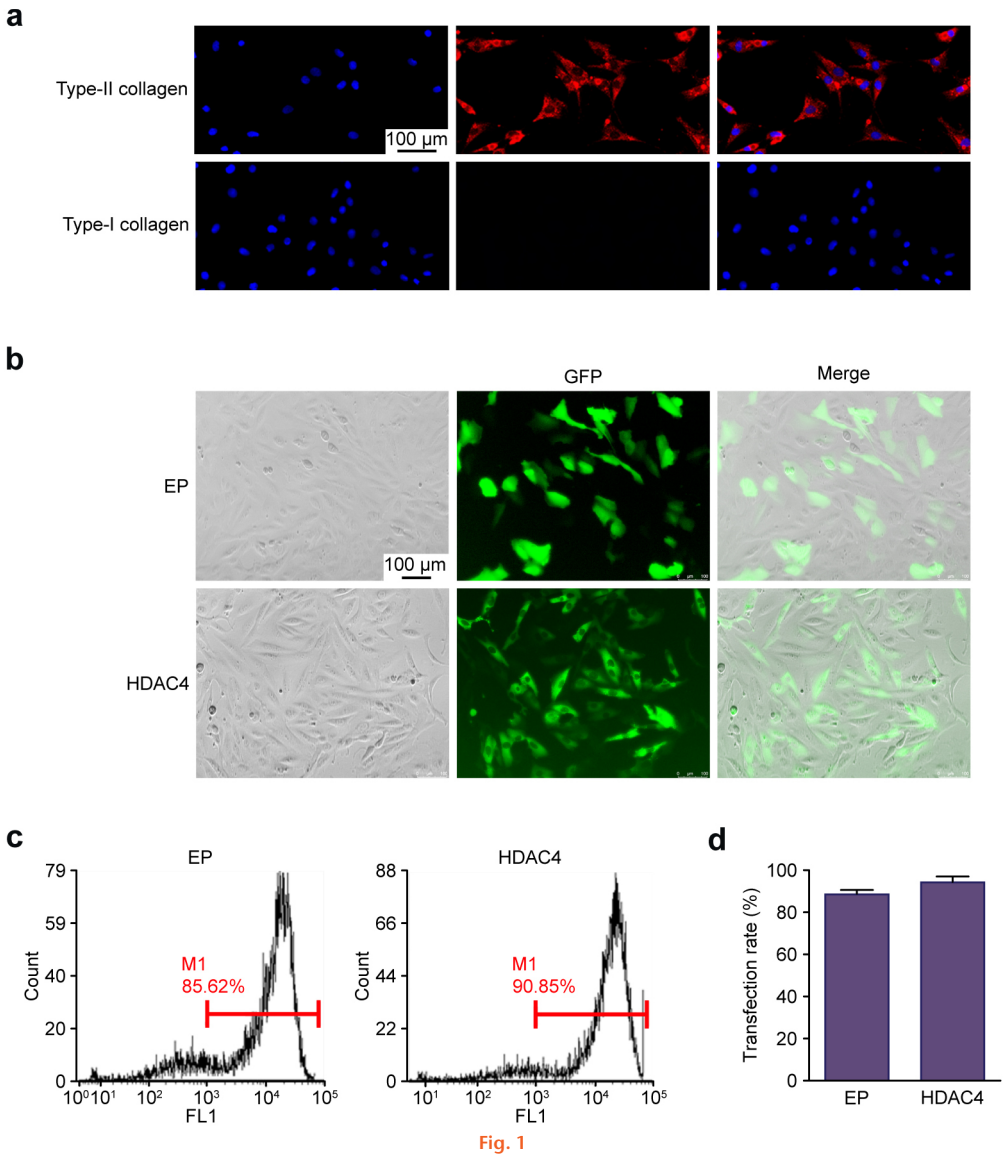

Fig. 1

a) Immunofluorescence assay results showed that cells were positive for type II collagen (red) and negative for type I collagen (red, scale bar: 100 μm). b) The transfection efficiency in each group was observed by fluorescence microscopy. The empty adenovirus (EP) and histone deacetylase 4 (HDAC4) adenoviruses carried green fluorescent protein (GFP) (green); scale bar: 100 μm. c) Representative transfection rate of groups at 48 hours after transfection by flow cytometry. d) Data were quantified by the mean transfection rate (n = 3). FL1, FITC channel; M1, FITC positive cell rate.

Cell proliferation assays. Cell proliferation was detected using a Cell-Light EdU Kit (RiboBio, China) according to the manufacturer's protocol. EdU was added to the culture medium at a concentration of 50 μM. The cells were fixed with 4% paraformaldehyde, permeabilized with 0.5% Triton X-100 in phosphate-buffered saline (PBS) for 15 minutes, and subsequently incubated with Apollo reaction cocktail (containing Apollo reaction buffer, Apollo catalyst, Apollo 567 fluorescent dyes, and buffer additives) and Hoechst 33342 for 30 minutes away from light. The cells were then observed immediately under a fluorescence microscope (Olympus). The percentage of positive cells (red) was determined.

Western blotting. For verification of the results of RNA-seq in vitro, cells were plated at 50% to 60% confluence and grown until they reached 70% to 90% confluence after 24 hours. Then the cells were randomly divided into three groups: the control; interleukin (IL)-1β (10 ng/ml); and IL-1β+ HDAC4 groups. IL-1β was used to induce the OA chondrocyte models.[15] Then 48 hours after treatment, total protein from the chondrocytes was isolated and quantified by a Bradford Protein Assay Reagent Kit (Bio Rad Laboratories, USA). A total of 20 μg of total protein was separated by 10% sodium dodecyl-sulfate polyacrylamide gel electrophoresis (SDS–PAGE) under reducing conditions. The proteins were then transferred onto a nitrocellulose (NC) filter membrane (Bio Rad Laboratories) and probed with polyclonal antibodies against HDAC4 (B-5) (SC-365093; Santa Cruz Biotechnology, USA), HDAC4 (A-4) (SC-46672; Santa

Cruz Biotechnology), CCR4-NOT Complex subunit 1 (CNOT1) (A5969; ABclonal, China), and glyceraldehyde 3-phosphate dehydrogenase (GAPDH) (ab5174; Abcam, UK). The secondary antibodies IRDye 800CW goat anti-rabbit (red) (ab216773) or IRDye 680RD goat anti-mouse (green) (ab216776; both Abcam, UK) diluted at a ratio of 1:5,000 in PBS-Tween (PBS-T) were used. The immunoreactive proteins were visualized using Odyssey CLx, and band densities were quantified using Empiria Studio Analysis software (both LI-COR Biosciences, Germany).

The total protein of human cartilage explants was isolated and quantified by a Bradford Protein Assay Reagent Kit (Bio Rad Laboratories) and prepared for Western blotting. The Western blotting protocol and the indicators were the same as those in the above cell experiments.

RNA-seq analysis of chondrocytes. The procedure for RNA-seq was modified based on previously published methods.[16] Briefly, total RNA was extracted from chondrocytes of the EP, wild-type HDAC4 (WT-H4), and mutated HDAC4 (M-H4) transfection groups 48 hours after transfection using TRIzol reagent (Invitrogen). RNA degradation and contamination were evaluated on 1% agarose gels. RNA purity was assessed using a NanoPhotometer spectrophotometer (Implen, USA), RNA concentration was measured using a Qubit RNA Assay Kit in Qubit 2.0 Fluorometer (Life Technologies; Thermo Fisher Scientific, USA), and RNA integrity was assessed using the RNA Nano 6000 Assay Kit of the Bioanalyzer 2100 system (Agilent Technologies).

According to the manufacturer's instructions, the sequencing library was constructed using the NEB Next Ultra RNA Library Prep Kit for Illumina (New England Biolabs (NEB), USA). The index of the reference genome was built using HISAT2 v2.0.5. Differential expression analysis between groups was determined using the DESeq2 R package v1.22.1 (R Foundation for Statistical Computing, Austria). All statistical analyses were conducted using the R statistical programming language (R Foundation for Statistical Computing). Genes with an adjusted p-value of < 0.05 found by DESeq2 were considered differentially expressed. Differentially expressed genes (DEGs) were defined as having a fold change (FC) ≥ 2 and p-value ≤ 0.05. Gene Ontology (GO) enrichment analysis and Kyoto Encyclopedia of Genes and Genomes (KEGG) pathway analysis were performed using the clusterProfiler R package v4.0 (R Foundation for Statistical Computing). Gene set enrichment analysis (GSEA) was performed using all normalized probes on the 'curated gene set' and 'GO gene set' collections of the Molecular Signatures Database v5.2 (MSigDB).[17]

Real-time quantitative PCR. Total RNA was isolated from human chondrocyte groups using the RNeasy Isolation Kit (Qiagen, USA). Total RNA (1 µg) was reverse-transcribed to complementary DNA (cDNA) using a reverse transcription kit (TaKaRa, Japan). The resulting cDNA (80 ng/µl) was used as a template to quantify the relative content of messenger RNA (mRNA) using a QuantiTect SYBR Green PCR Kit (TaKaRa) with a QuantStudio 6 Flex Fluorescence Detection System (Thermo Fisher Scientific). The primer pairs used are listed in Table I. Relative transcript levels were calculated according to the equation $x = 2^{-\Delta\Delta Ct}$, where ΔΔCt = ΔCt E - ΔCt C (ΔCt E = Ct exp - Ct 18 S, ΔCt C = Ct C - Ct18S).

Table I. Primers used in this study with the species (human), name, orientation, and sequence used in quantitative polymerase chain reaction.

Name	Forward/reverse	Sequence (5' to 3')
	Forward	CGGCTACCACATCCAAGGAA
18S	Reverse	GCTGGAATTACCGCGGCT
	Forward	GATTCAGGAGTGTGCGTTGC
CNOT1	Reverse	TGGGCAGCGAAACCTCTAAG
	Forward	TTTGACATCTTTGAACTCACCG
THBS1	Reverse	AGAAGGAGGAAACCCTTTTCTG
	Forward	GTCTATACTTACTGCCAGCG
SEMA5A	Reverse	GTTAAATGCCTTGATGGCCTC
	Forward	GATTCGCATGTGCAAGGACC
PRPF8	Reverse	TTGCCAAGCCATCGCTCTAA
	Forward	ATGGCCCTACGCTACCCTAT
RPL36	Reverse	AATCATGTCCCGCACGAACT
	Forward	ATGGACACCAGCCGTGTG
RPS28	Reverse	TCAGCGCAACCTCCGGGCTT
	Forward	GCCTGCCACCTCCTATGTG
RPL28	Reverse	TCTCCAGCCCATATTGCAACC
	Forward	CGCGCTACTTTGGGATAAAG
POLR2E	Reverse	ACCAGCCGGTAGGTGATGTA;
	Forward	GCGTCCCAAGAAGAAGGTCA
UBA52	Reverse	ACCAATTGCTGCTCCAGTCA
	Forward	AGTGGACATCCGCCATAACAA
RPL18	Reverse	CTTGACCAACAGCCTCAGGTA

CNOT1, CCR4-NOT transcription complex subunit 1; POLR2E, RNA polymerase II polypeptide E; PRPF8, pre-messenger RNA (mRNA) processing factor 8; RPL18, ribosomal protein L18; RPL28, ribosomal protein L28; RPL36, ribosomal protein L36; RPS28, ribosomal protein S28; 18S, 18S ribosomal RNA; SEMA5A, Semaphorin 5A; THBS1, Thrombospondin 1; UBA52, ubiquitin A-52 residue ribosomal protein fusion product 1.

The verification of RNA-seq in vivo: a pilot study. Two-month-old male Sprague Dawley (SD) rats (180 to 230 g, n = 30) were obtained from the Experimental Animal Centre (Shanxi Medical University, China). The rats were randomized to three groups (n = 10 per group): sham operation (control); anterior cruciate ligament transection (ACLT) alone; and ACLT and HDAC4 adenovirus (1×10^{11} PFU/ml). ACLT and sham operations were performed on the right knees as described previously.[18] HDAC4 adenovirus (40 µl) was used to treat rat post-traumatic OA by intra-articular injection. The treatment was performed 24 hours after ACLT and then once every three weeks for eight weeks. All animals were euthanized at eight weeks after the operation.

The extent of OA progression was evaluated using Safranin O, and the protein expression of CNOT1 was detected by immunohistochemical staining. The ARRIVE checklist for the design and execution of protocols for

animal research and treatment was used and is included in the Supplementary Material.

Histology. The human cartilage explants were fixed in 10% formalin (MilliporeSigma) for 72 hours. The specimens were decalcified in Richman-Gelfand-Hill solution, processed in a Tissue-Tek VIP 1000 tissue processor (Miles Laboratories, USA), and embedded in a single block of Paraplast X-tra (Thermo Fisher Scientific, USA). Blocks were trimmed to expose the tissue using a rotary microtome (Leica RM2125; Leica Microsystems, Germany). Ten adjacent sections were collected at intervals of 0 µm, 100 µm, and 200 µm. Two serial 6 µm-thick sections from each interval were stained with Safranin O.

In the in vivo study, the femora and tibiae of SD rats were hemisected in the midsagittal plane, and each half was embedded in a single block of Paraplast X-tra. Blocks were trimmed to expose the cartilage. Ten adjacent sections were collected at intervals of 0 µm, 100 µm, and 200 µm (Leica RM2125). Two serial 6 µm-thick sections from each interval were stained with Safranin O.

Immunohistochemistry. To detect the distribution of CNOT1 in cartilage, we carried out immunohistochemistry using the 3,3'-diaminobenzidine (DAB) Histostain streptavidin peroxidase (SP) kit (Novex, Life Technologies, USA). The sections (6 µm) were deparaffinized and rehydrated using conventional methods. The sections were digested with 5 mg/ml hyaluronidase in PBS (Millipore Sigma, USA) at 37°C for ten minutes. Endogenous peroxidase was blocked by treating the sections with 3% hydrogen peroxide in methanol (Millipore Sigma) at room temperature for ten minutes. Non-specific protein binding was blocked by incubation with a serum blocking solution (LI-COR Biosciences) at room temperature for ten minutes. The sections were incubated with specific antibodies against rat CNOT1 (A5969; ABclonal) at 4°C overnight. Thereafter, the sections were treated sequentially with biotinylated secondary antibody and SP conjugates at 37°C for ten minutes and then developed in DAB chromogen (Invitrogen) for three minutes. The sections were counterstained with haematoxylin (Invitrogen) for one minute. Photomicrographs were obtained with a Nikon E800 microscope (Nikon, USA).

Statistical analysis. The data are presented as the mean (standard deviation (SD)) obtained from at least three independent experiments. Each experimental measurement was performed in triplicate. Two-tailed paired *t*-tests were used to compare changes in the gene expression and protein expression levels. A p-value less than 0.05 was considered statistically significant. Statistical analyses were performed using SPSS v18.0 (SPSS, USA).

Results

HDAC4 markedly improves the survival rate and biofunction of chondrocytes. At present, most studies on HDAC4 in cartilage focus on its inhibition of chondrocyte hypertrophy. In this study, the key markers (RUNX2, Col-X, and MMP-13) involved in the hypertrophic differentiation of chondrocytes were also detected by Western blotting four days after transfection. The results showed that HDAC4 treatment indeed significantly decreased the expression of RUNX2, Col-X, and MMP-13 compared to that of the EP group (Figure 2a). To investigate the other functions of HDAC4, we detected the chondrocyte survival rate by the real-time cell analysis (RTCA) assay 0 to 96 hours after transfection. Compared with that of the EP group, the cell index (live cell counts) of the HDAC4 transfection group was markedly higher (Figure 2b). The result was confirmed by an EdU assay (Figure 2c). The flow cytometry analysis results showed that the cell survival rates in the EP and HDAC4 transfection groups were 83.3% and 93.6%, respectively (Figure 2d). In contrast, the early cell apoptosis rate of the HDAC4 group decreased significantly (Figure 2d). All these results indicated that HDAC4 could not only inhibit the hypertrophic differentiation of chondrocytes, but also effectively improve the survival rate of chondrocytes by promoting proliferation and inhibiting apoptosis.

Differential gene expression and GO analysis (EP versus HDAC4). For determination of the molecular mechanism of HDAC4 in chondrocytes, human chondrocytes were collected and treated with EP and HDAC4 for 70 hours separately, and the cells were then subjected to RNA-seq (Supplementary Figure ba). The mRNA levels of *HDAC4* were detected and found to be six-fold higher in the HDAC4 transfection groups than in the EP group (Supplementary Figure bb). A volcano plot was drawn to compare DEGs between the two groups (Figure 3a), and the results showed that HDAC4 induced 2,668 significant gene expression changes in chondrocytes (1,483 genes upregulated and 1,185 genes downregulated; Figure 3b and Supplementary Table i).

To learn more about the biological effects of HDAC4 based on the differential gene regulation in chondrocytes, we performed GO enrichment analysis for different treatment groups. Between the EP and HDAC4 groups, GO analysis showed multiple terms ($p < 0.05$; Supplementary Table ii). The top ten GO terms are shown in Figure 3c, including cellular macromolecule catabolic process, cell cycle, apoptotic process, and autophagy.

KEGG pathway analysis of DEGs (EP versus HDAC4). The DEGs were matched to the Kyoto Encyclopedia of Genes and Genomes (KEGG) database under the different treatments. For EP versus HDAC4, we identified 21 pathways ($p < 0.05$; Supplementary Table iii). The top ten KEGG pathways are shown in Figure 4a, and the results showed that five signalling pathway terms were important: ribosome, oxidative phosphorylation, focal adhesion, thyroid hormone signalling pathway, and oestrogen signalling pathway. Subsequently, the enhanced KEGG pathways were analyzed, and the top ten pathways are shown in Figure 4b. Ribosomes exhibited an increased degree of upregulation (we have indicated the ribosome signalling in Figure 4b).

RNA-seq analysis (EP versus mutated HDAC4). Nucleocytoplasmic trafficking is considered an important element in controlling the transcriptional

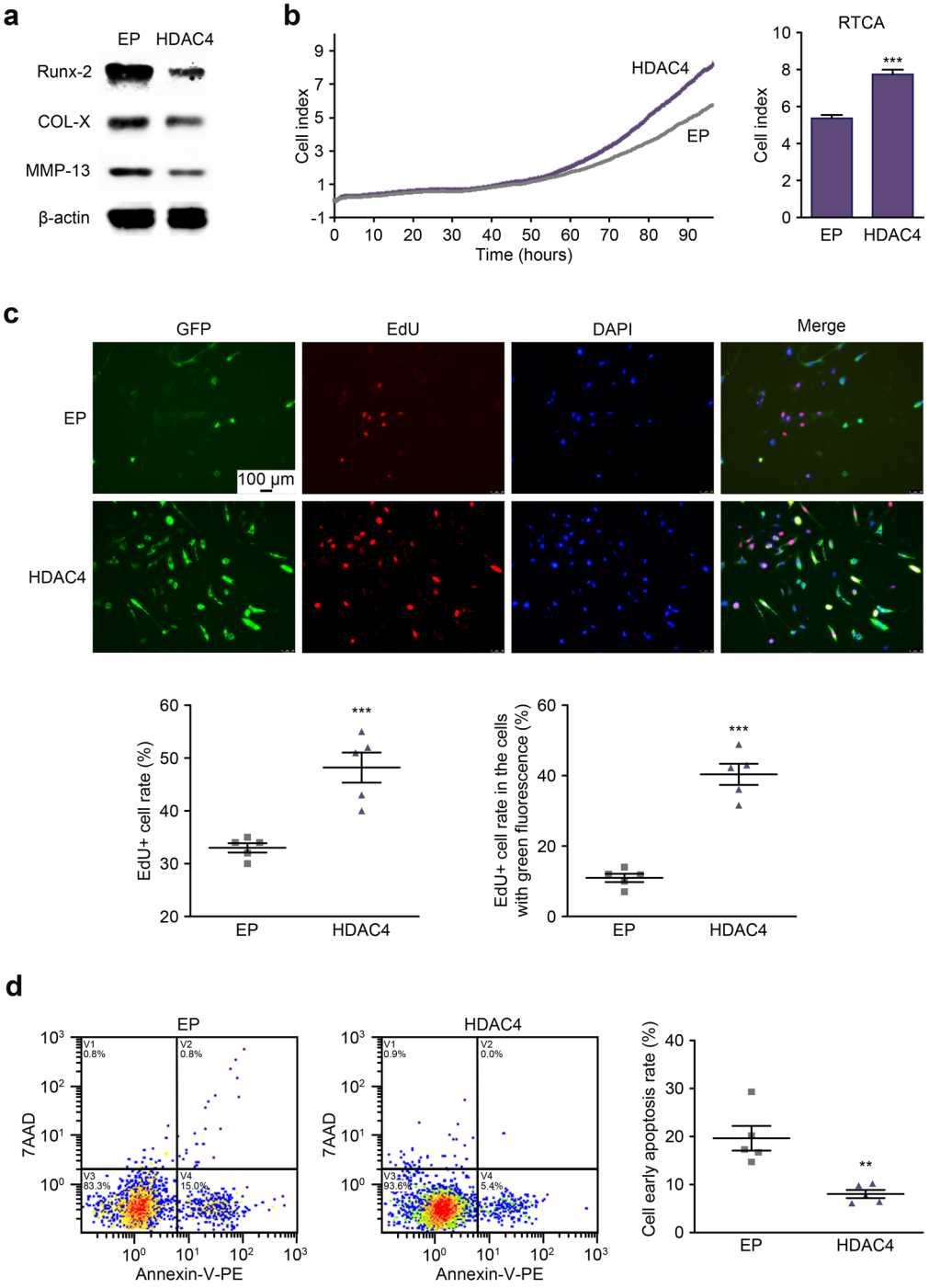

Fig. 2

Histone deacetylase 4 (HDAC4) markedly improves the survival rate and biofunction of chondrocytes. a) Representative protein expression levels of runt-related transcription factor 2 (RUNX2), type X collagen (Col-X), matrix metallopeptidase-13 (MMP-13), and β-actin in chondrocytes. b) Representative cell survival rates of groups were detected by real-time cell analysis (RTCA) assay; the HDAC4 group (purple) and the empty adenovirus (EP) group (grey), the data were quantified by mean cell index (CI) (n = 4). c) Representative EdU-based cell proliferation assay results. The EdU-positive cells showed red fluorescence. Scale bar: 50 μm. The percentage of EdU-positive cells in all cells and the percentage of EdU-positive cells in the cells with red fluorescence were quantified. d) Cell viability was detected by flow cytometry; of the four regions in the figure, zone V3 indicates negative 7-amino-actinomycin (7-AAD) and Annexin-V-phycoerythrin (PE) staining, showing the percentage of living cells, while zone V4 indicates negative 7-AAD staining and positive Annexin-V-PE staining, showing the percentage of early apoptosis cells. The data were quantified by the early apoptosis rate (n = 6). Data are expressed as the mean (standard deviation). ***p < 0.001. DAPI, 4′,6-diamidino-2-phenylindole; GFP, green fluorescent protein.

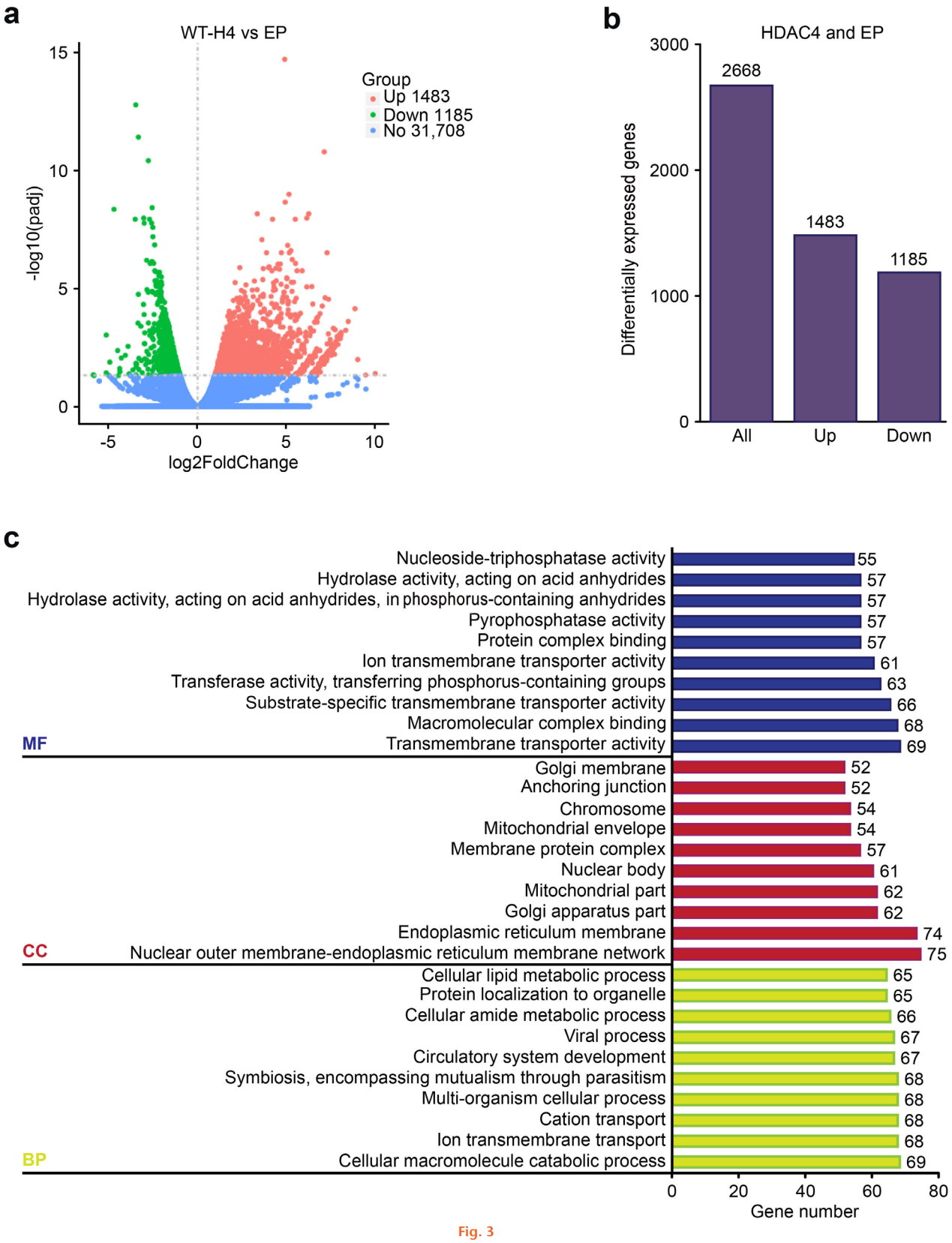

Fig. 3

a) Volcano plot of the differentially expressed genes (DEGs) for empty adenovirus (EP) versus histone deacetylase 4 (HDAC4, wild-type (WT)-H4). The genes that were found to be statistically significant (false discovery rate ≤ 0.05) are highlighted. b) The bar chart shows the total DEGs, upregulated DEGs, and downregulated DEGs. c) Gene Ontology (GO) functional enrichment analysis of DEGs with or without HDAC4. BP, biological process; CC, cell component; MF, molecular function.

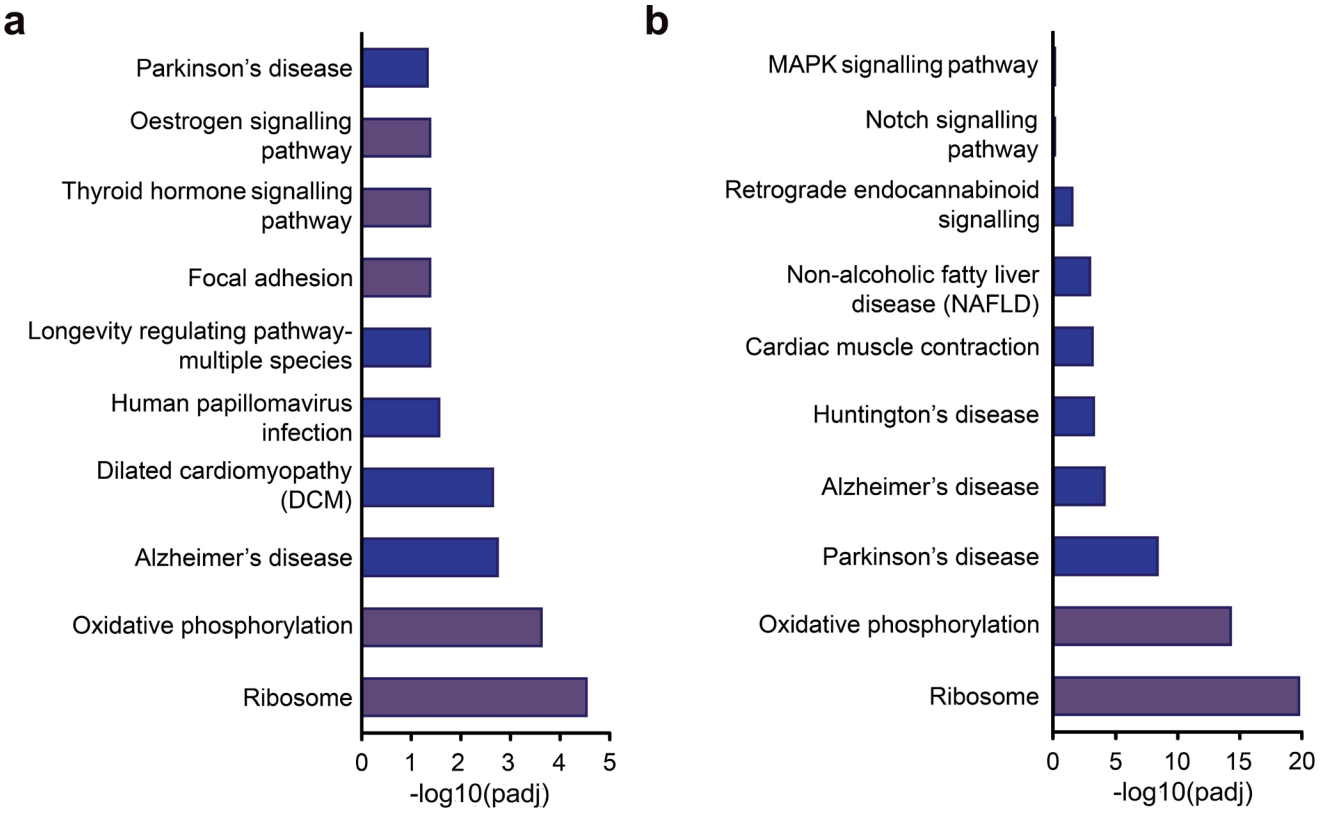

Fig. 4

a) Kyoto Encyclopedia of Genes and Genomes (KEGG) pathway enrichment analysis of differentially expressed genes (DEGs) with or without histone deacetylase 4 (HDAC4). b) KEGG pathway enrichment analysis of upregulated DEGs with or without HDAC4. MAPK, mitogen-activated protein kinase; padj, p-adjusted.

repression function of HDAC4. In the nucleus, HDAC4 could partner with histones and/or transcription factors to inhibit transcription. In contrast, cytoplasmic accumulation of HDAC4 removes the repression of transcription.[19] As early as the year 2000, Wang et al[20] and Grozinger and Schreiber[21] discovered that inhibiting the interaction between HDAC4 (Ser-246, Ser-467, and Ser-632) and 14-3-3 protein in the cytoplasm could significantly increase the function of HDAC4 by anchoring HDAC4 in the nucleus. Moreover, according to the current view, HDAC4 protein can be cleaved by caspase-2/3 at the Asp-289 site in chondrocytes, which significantly decreases the expression of HDAC4 in chondrocytes, including the nucleus.[22] Therefore, in this study, the A289E/S246/467/632 A sites of HDAC4 were mutated to amplify the function of HDAC4 by increasing the expression of HDAC4 in the nucleus, and RNA-seq was performed to further investigate the molecular mechanism of HDAC4 in chondrocytes.

To evaluate the expression of HDAC4 in the nucleus, we observed the subcellular location of HDAC4 by fluorescence microscopy. The results showed that: in the HDAC4 group, HDAC4 was mainly located in the cytoplasm; in the HDAC4+ caspase inhibitor group, HDAC4 was located in both the cytoplasm and nucleus; and in the mutated HDAC4 group, HDAC4 was mainly located in the nucleus (Supplementary Figure aa). The results were confirmed by Western blotting (Supplementary Figures ab and ac). To investigate the function of mutated HDAC4, we determined the chondrocyte survival rate by the RTCA assay during 0 to 70 hours after transfection. Compared with that of the other groups, the cell index (live cell counts) of the mutated HDAC4 transfection group was markedly higher (Supplementary Figures ca and cb), and the result was confirmed by detecting the total protein levels in the groups at 70 hours after transfection (Supplementary Figure cc). The above results indicate that mutating the A289E/S246/467/632 A sites of HDAC4 could amplify the function of HDAC4 by increasing HDAC4 expression in the nucleus.

The RNA-seq analysis showed that mutated HDAC4 induced 821 DEGs in chondrocytes, including 469 upregulated genes and 332 downregulated genes (Figure 5a and Supplementary Table iv). GO analysis showed the multiple terms ($p < 0.05$, Supplementary Table v). The top ten GO terms are shown in Figure 5b. Importantly, in the biological process (BP), 43 genes were enriched in the term mRNA metabolic process. In the terms of cellular component (CC), 38 genes were enriched in the term nucleolus, 37 genes were enriched in ribonucleoprotein complex, 14 genes were enriched in ribosome, and 11 genes were enriched in ribosomal subunit. In the terms of molecular function (MF), 30

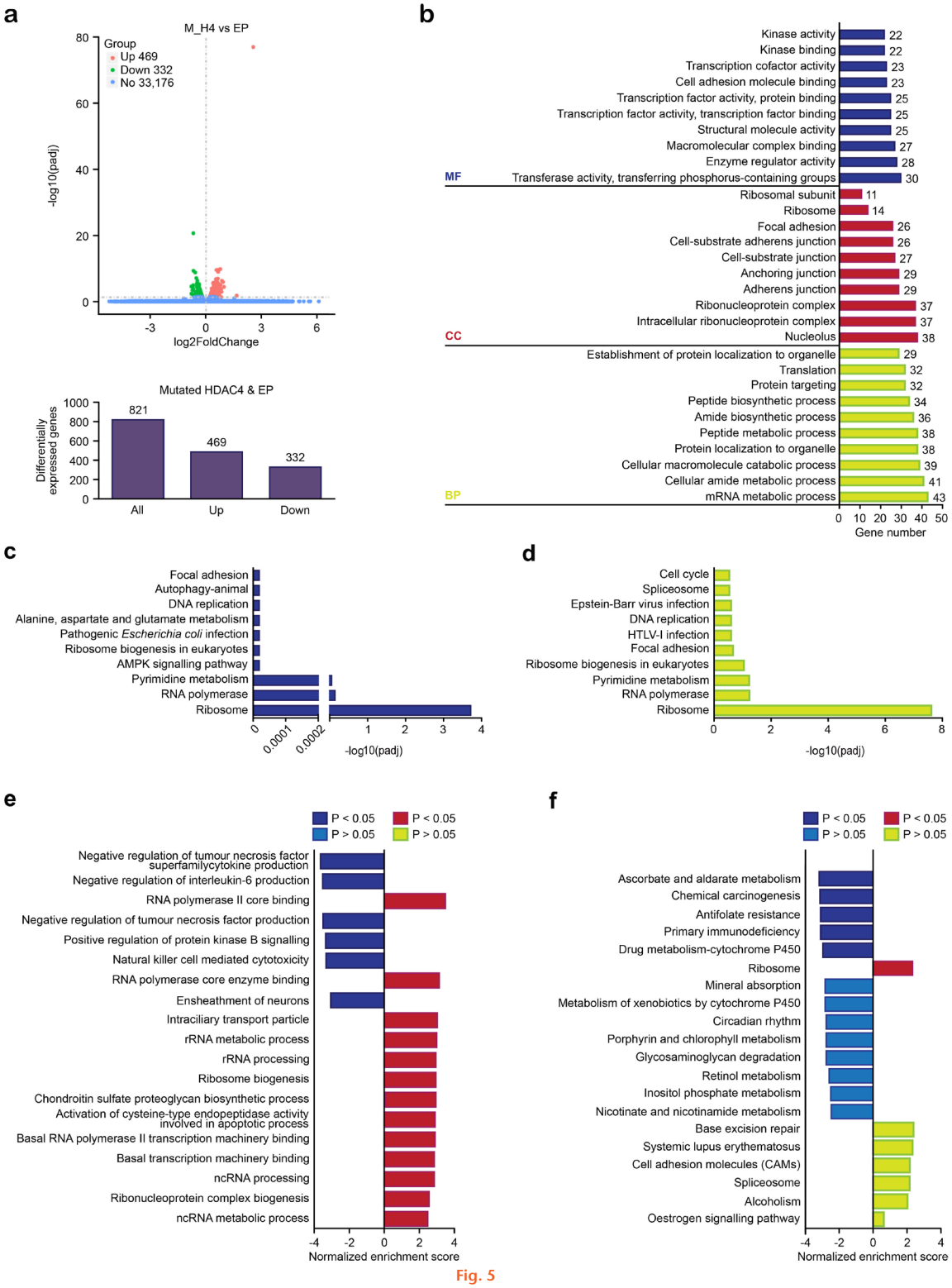

Fig. 5

a) Volcano plot of the differentially expressed genes (DEGs) for empty adenovirus (EP) versus mutated histone deacetylase 4 (M_H4). The genes that were found to be statistically significant (false discovery rate ≤ 0.05) are highlighted; the bar chart shows the total DEGs, upregulated DEGs, and downregulated DEGs. b) Gene Ontology (GO) functional enrichment analysis of DEGs with or without mutated HDAC4. c) Kyoto Encyclopedia of Genes and Genomes (KEGG) pathway enrichment analysis of DEGs between the EP and mutated HDAC4 groups. d) KEGG pathway enrichment analysis of upregulated DEGs between the EP and mutated HDAC4 groups. e) Gene set enrichment analysis (GSEA) based on GO enrichment analysis showed the upregulated (red) and downregulated pathways (blue) comparing the mutated HDAC4 and EP groups. f) GSEA based on KEGG enrichment analysis comparing the mutated HDAC4 and EP groups. AMPK, AMP-activated protein kinase; BP, biological process; CC, cellular component; HTLV-I, human T-lymphotropic virus type 1; MF, molecular function; mRNA, messenger RNA; ncRNA, non-coding RNA; padj, p-adjusted; rRNA, ribosomal RNA.

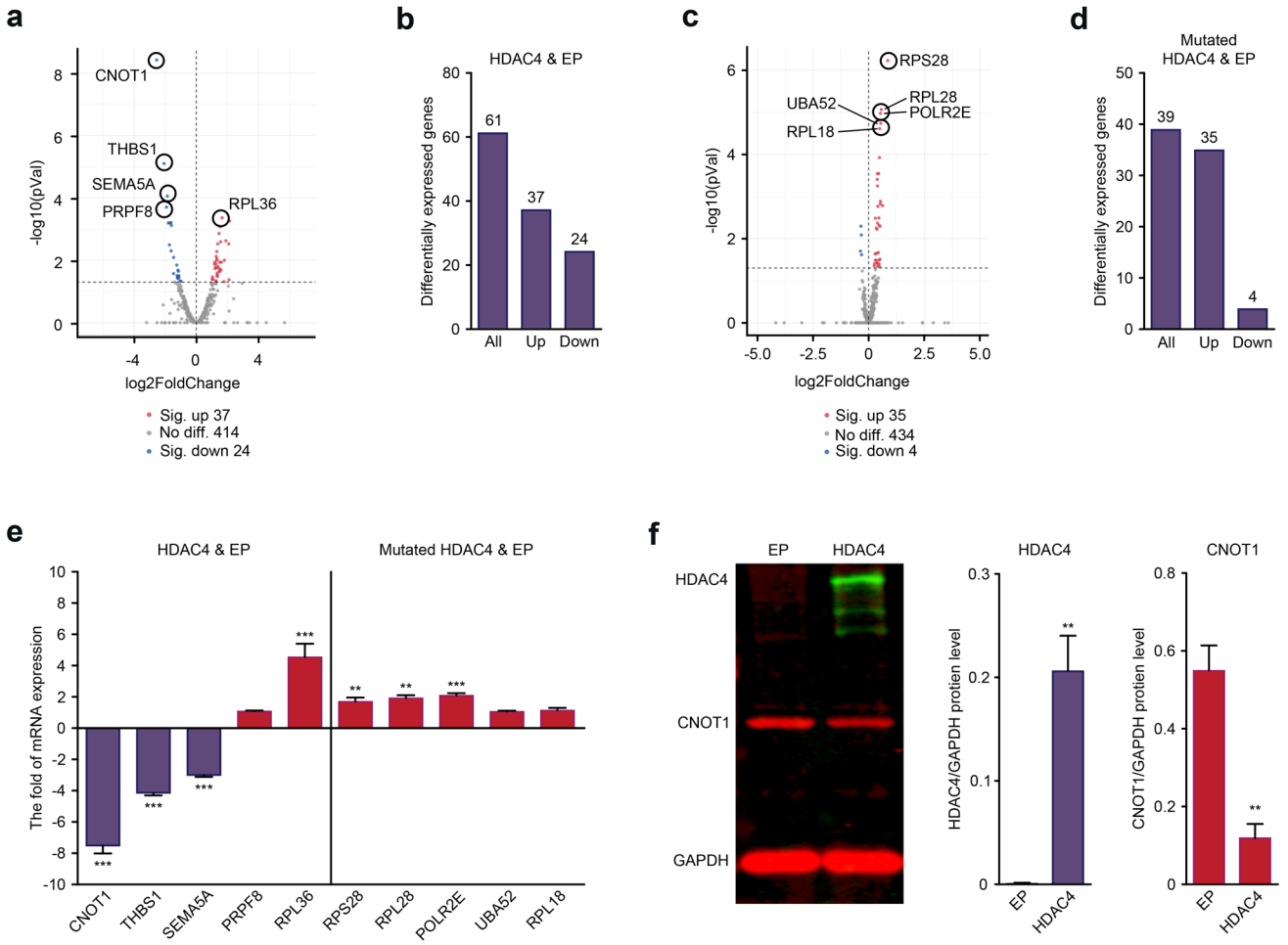

Fig. 6

a) Volcano plots showing the differentially expressed genes (DEGs) of the ribosome pathway in the histone deacetylase 4 (HDAC4) groups and the genes that were found to be statistically significant (false discovery rate (FDR) ≤ 0.05). b) All DEGs, upregulated genes, and downregulated genes. c) Volcano plots showing the DEGs of the ribosome pathway in the HDAC4 groups, the genes that were found to be statistically significant (FDR ≤ 0.05). d) All DEGs, upregulated genes, and downregulated genes. e) Validation of the top ten genes by polymerase chain reaction (PCR) (n = 6). f) Validation of the top gene (CNOT1) by Western blotting (n = 3). The data are expressed as the mean (standard deviation). **p < 0.01, ***p < 0.001. GAPDH, glyceraldehyde 3-phosphate dehydrogenase.

genes were enriched in transferase activity and transferring phosphorus-containing groups, 27 genes were enriched in macromolecular complex binding, 25 genes were enriched in transcription factor activity and transcription factor binding, and 23 genes were enriched in transcription cofactor activity. All of the above terms were closely related to three keywords: nucleus, transcription function, and ribosome.

KEGG pathway analysis identified ten pathways ($p < 0.05$; Supplementary Table vi) (Figure 5c), and the ribosome pathway was the pathway with the most significant change. The result was confirmed by the enhanced KEGG pathway analysis (Figure 5d). GSEA was performed. Unlike GO/KEGG enrichment analysis, which only focuses on significantly upregulated or downregulated genes with the omission of some genes with insignificant differential expression but important biological function, GSEA is based on the whole gene set. Here, the GSEA of GO enrichment showed that the terms closely related to ribosome, RNA polymerase II core binding, RNA polymerase core enzyme binding, ribosomal RNA (rRNA) metabolic process, rRNA process, and ribosome biogenesis were significantly upregulated (Figure 5e and Supplementary Table vii). The GSEA of KEGG enrichment showed that the ribosome pathway was the only pathway that was significantly upregulated (Figure 5f and Supplementary Table viii).

In vitro and in vivo validation. To validate the results of RNA-seq, we analyzed the ribosome-related genes for EP versus HDAC4 and EP versus mutated HDAC4. The volcano plot of the DEGs showed that HDAC4 induced 61 significant gene expression changes (37 genes upregulated and 24 genes downregulated), and the top five DEGs were *CNOT1, THBS1, SEMA5A, PRPF8, and RPL36* (Figures 6a and 6b). Mutated HDAC4 induced 39 significant gene expression changes (35 genes upregulated and four genes downregulated), and the top five DEGs were *RPS28, RPL28, POLR2E, UBA52, and RPL18* (Figures 6c

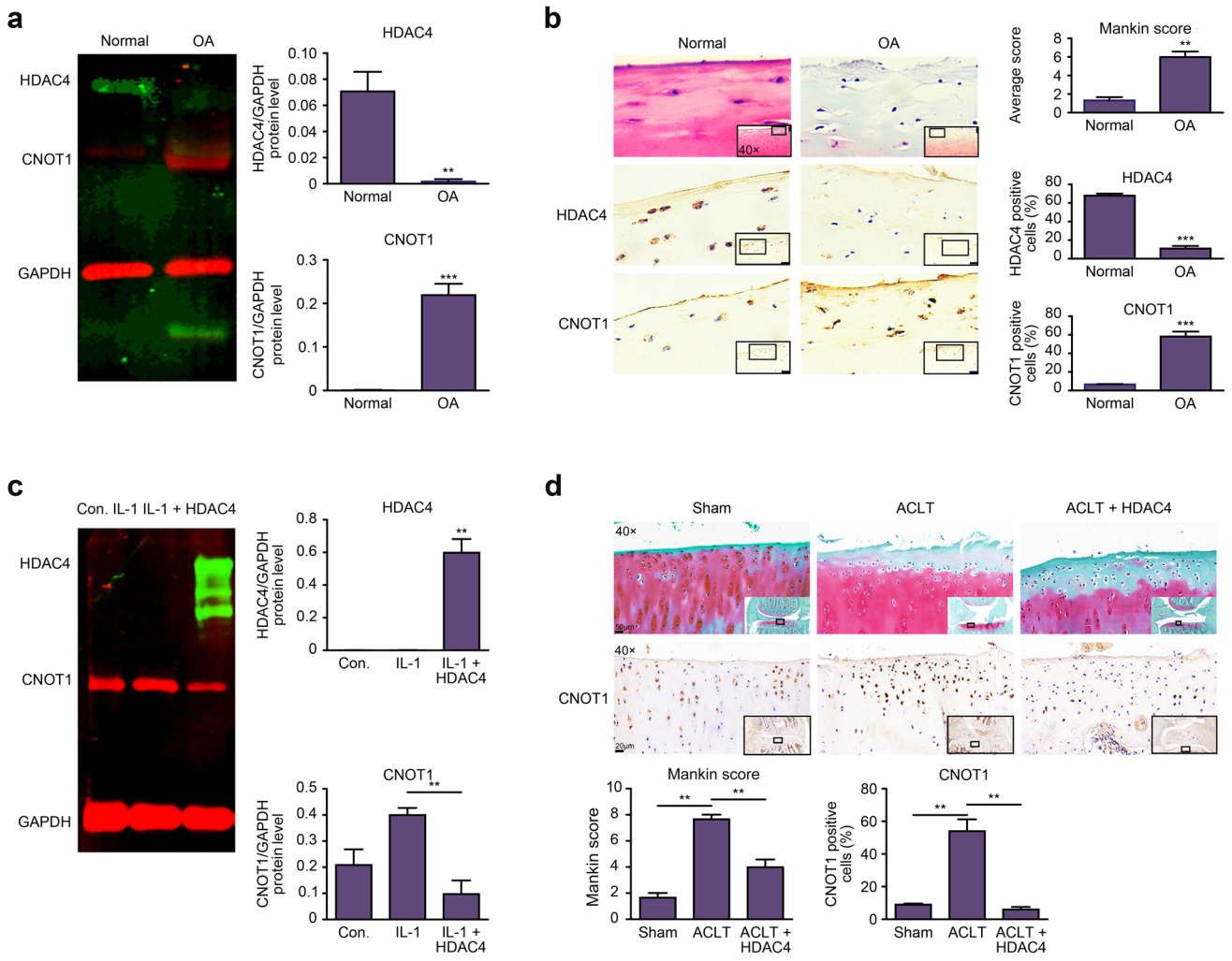

Fig. 7

a) The protein level of CNOT1 in normal and osteoarthritis (OA) cartilage tissue was detected by Western blotting (n = 3). b) The protein expression of CNOT1 in relatively normal and OA cartilage tissue was detected by immunohistochemistry (n = 3). c) Western blotting results showed the protein level of CNOT1 in the OA chondrocyte model (n = 3). d) Safranin O and fast green staining showed the degenerative degree of cartilage tissue, and immunohistochemistry results showed the protein expression of CNOT1 in OA rat models (n = 10). The data are expressed as the mean (standard deviation). **p < 0.01, ***p < 0.001. ACLT, anterior cruciate ligament transection; Con., control; IL, interleukin; GAPDH, glyceraldehyde 3-phosphate dehydrogenase; HDAC4, histone deacetylase 4.

and 6d). Real-time Quantitative PCR Detecting System (QPCR) was used to validate the expression of the ten chosen genes. The results showed that except for *PRPF8, UBA52,* and *RPL18*, significant changes were found in the other seven genes, with a FC > 2.0. Among the ten genes, *CNOT1* exhibited a higher degree of downregulation (FC approximately 7.5) (Figure 6e). The Western blotting results of CNOT1 were consistent with the qPCR results: overexpression of HDAC4 decreased the protein level of CNOT1 in chondrocytes (Figure 6f).

To further validate the RNA-seq results, we assayed the expression of HDAC4 and CNOT1 in normal and OA human cartilage tissues by Western blotting and immunohistochemistry. The results showed that HDAC4 protein levels were decreased in OA cartilage tissues, whereas CNOT1 protein levels were increased (Figures 7a and 7b). Subsequently, HDAC4 was used to treat OA chondrocyte models induced by IL-1β, and the results showed that HDAC4 effectively downregulated the expression of CNOT1 in the OA chondrocyte models (Figure 7c). The in vivo experiments showed the same result: intra-articular injection of a HDAC4 adenovirus effectively decreased the expression of CNOT1 in cartilage tissues of OA rats (Figure 7d).

Discussion

HDAC4 plays a key role in the control of gene transcription, which has been associated with various signalling networks of development in the skeletal muscle,[23] brain,[24] heart,[25] vascular system,[26] liver,[27] and cartilage,[28] even in adulthood, enabling adaptation to environmental changes.[29] However, the molecular mechanism of HDAC4 is still unclear. This study discovered novel molecular mechanisms of HDAC4 in chondrocytes via HDAC4

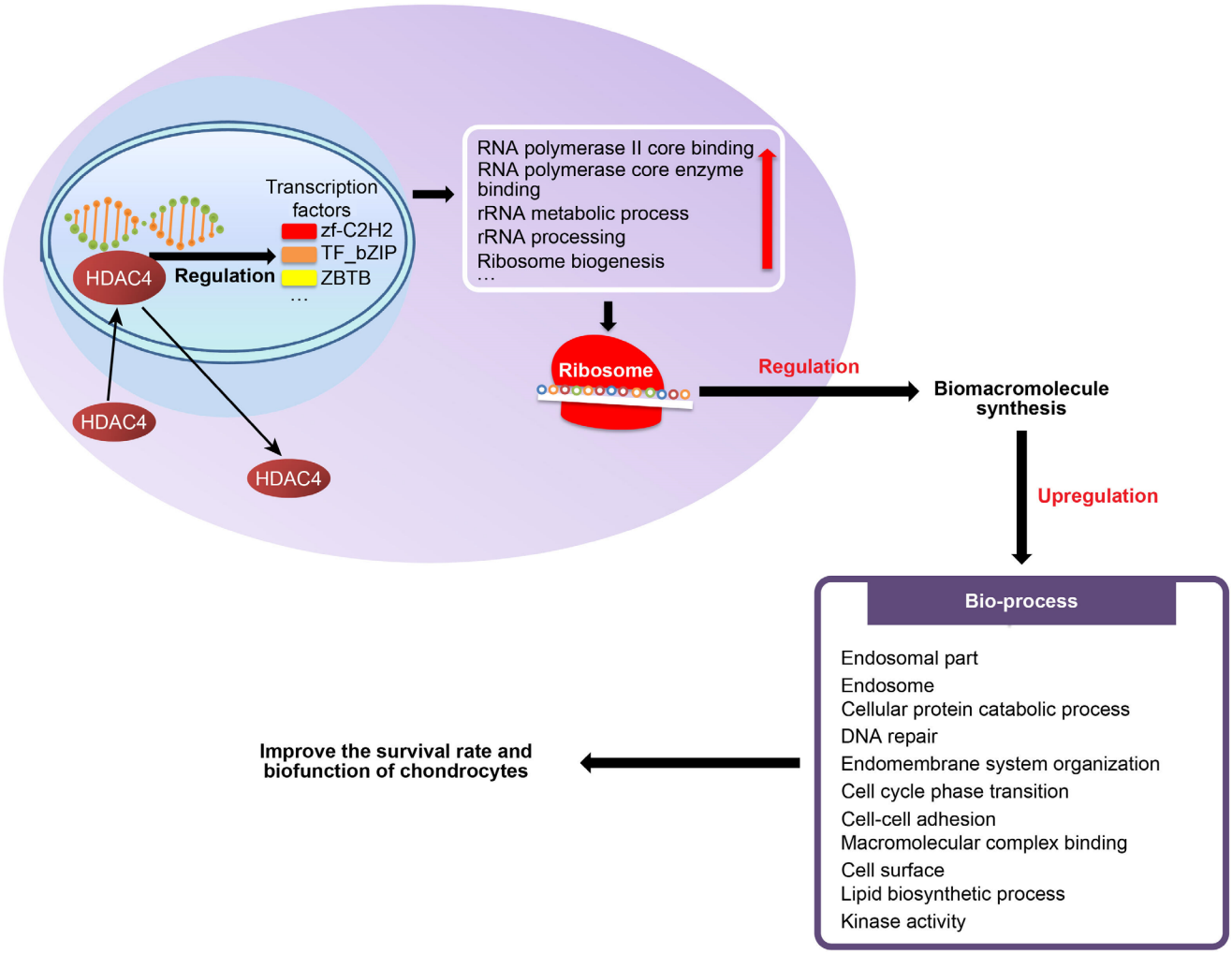

Fig. 8

Hypothesis schematic of the molecular mechanism by which histone deacetylase 4 (HDAC4) improves the survival rate and biological function of chondrocytes. rRNA, ribosomal RNA; TF_bZIP, transcription factor_basic leucine zipper zinc finger; ZBTB, BTB domain; zf-C2H2, zinc finger-C2H2.

mutagenesis and RNA-seq analysis. The results showed that the enhanced ribosome pathway played a key role in HDAC4 improving the survival rate and biofunction of chondrocytes.

The eukaryotic ribosome, a translational machinery, is believed to be responsible for protein synthesis from mRNAs and consists of four rRNA species and 79 ribosomal proteins (RPs). Three RNA polymerases are involved in the process called ribosome biogenesis, including RNA polymerase I, II, and III. Ribosome biogenesis is an extraordinarily complex process that is essential for cell growth, proliferation, differentiation, and animal development.[30,31] In the present study, the RNA-seq results showed different transcriptomic profiles in the HDAC4 group (Figures 3a and 3b). The GO enrichment analysis showed that HDAC4 significantly influenced the BP, CC, and MF in chondrocytes, which indicated that the effect of HDAC4 in chondrocytes was not achieved by inhibiting hypertrophy differentiation alone (Figure 3c). Interestingly, in KEGG pathway enrichment analysis, ribosome-related pathways showed the most significant change for EP versus HDAC4 and EP versus mutated HDAC4 (Figures 4, 5c, and 5d). In particular, GSEA for EP versus mutated HDAC4 revealed that the terms closely related to ribosome function, RNA polymerase II core binding, RNA polymerase core enzyme binding, rRNA metabolic process, rRNA process, and ribosome biogenesis were significantly enhanced (Figure 5e), and the ribosome pathway was the only one significantly enhanced by mutated HDAC4 (Figure 5f). All these results imply that upregulation of the ribosome pathway might be crucial in HDAC4 regulation of the chondrocyte survival rate and biofunction.

To further confirm the above conclusion, we validated the expression of the ten chosen genes related to ribosomes by qPCR. The results showed that except for *PRPF8*, *UBA52*, and *RPL18*, the other DEGs showed a trend of change that was consistent with the sequencing results, and *CNOT1* exhibited a higher degree of downregulation (Figure 6). Thus, we examined the effect of

HDAC4 regulation of CNOT1 in normal chondrocytes, OA chondrocytes, and OA rat models. The results suggested that overexpression of HDAC4 effectively decreased the protein levels of CNOT1 in both normal chondrocytes and OA models (Figure 7).

Additionally, we searched PubMed for research about ribosomes and HDAC4, and the results showed that Kappeler et al[32] found that histone deacetylase 6 associates with ribosomes and regulates de novo protein translation during arsenite stress. In 2021, Xu et al[33] discovered that histone deacetylases control lysine acetylation of RPs in rice. These results from other studies provided more evidence for the conclusion of this paper.[32,33]

Furthermore, HDAC4 is the key factor regulating gene transcription, and we profiled the effects of HDAC4 on transcription factors. The findings revealed the top three families, the transcription factor family of zinc finger-C2H2 (*zf-C2H2*), transcription factor_basic leucine zipper zinc finger (*TF_bZIP*), and BTB domain (*ZBTB*). Studies have shown that the crystal structure of human HDAC4 contains a Zn^{2+} ion, which is required for the deacetylation of HDAC4.[34] The Zn^{2+} ion could bind to the zinc finger to regulate the function of the target protein. This phenomenon might be the reason that the transcription factors *zf-C2H2, TF_bZIP, and ZBTB HDAC4* changed significantly in the HDAC4 transfection groups (Supplementary Figure bc).

In conclusion, integrating the findings of the study we hypothesized that HDAC4 might enhance the ribosome pathway by regulating the activities of transcription factors such as *zf-C2H2, TF_bZIP,* and *ZBTB*. Consequently, with increased ribosome function, various biological syntheses and bioprocesses were regulated, which in turn improved the survival rate and biofunction of chondrocytes (Figure 8). During this process, enhanced ribosomal function played a crucial role. However, further experimental validation should be performed.

Supplementary material

Figures related to: transfection efficiency and subcellular localization of HDAC4 and mutant HDAC4 in chondrocytes; RNA-seq, the RNA expression of groups, and the changes in the transcription factor families; and cell survival rates of groups. Tables illustrating data related to: differentially expressed genes (DEGs); Gene Ontology (GO) and Kyoto Encyclopedia of Genes and Genomes (KEGG) pathway analyses for empty adenovirus (EP) versus HDAC4 and EP versus mutated HDAC4; Gene Set Enrichment Analysis of GO enrichment analysis and KEGG enrichment analysis for EP versus mutated-HDAC4. An ARRIVE checklist is also included to show that the ARRIVE guidelines were adhered to in this study.

References

1. **Carballo CB**, **Nakagawa Y**, **Sekiya I**, **Rodeo SA**. Basic science of articular cartilage. *Clin Sports Med*. 2017;36(3):413–425.
2. **Charlier E**, **Deroyer C**, **Ciregia F**, **et al**. Chondrocyte dedifferentiation and osteoarthritis (OA). *Biochem Pharmacol*. 2019;165:49–65.
3. **Hussain SM**, **Neilly DW**, **Baliga S**, **Patil S**, **Meek RMD**. Knee osteoarthritis: a review of management options. *Scott Med J*. 2016;61(1):7–16.
4. **Parra M**. Class IIa HDACs - new insights into their functions in physiology and pathology. *FEBS J*. 2015;282(9):1736–1744.
5. **Vega RB**, **Matsuda K**, **Oh J**, **et al**. Histone deacetylase 4 controls chondrocyte hypertrophy during skeletogenesis. *Cell*. 2004;119(4):555–566.
6. **Arnold MA**, **Kim Y**, **Czubryt MP**, **et al**. MEF2C transcription factor controls chondrocyte hypertrophy and bone development. *Dev Cell*. 2007;12(3):377–389.
7. **Chen Z**, **Zhang Z**, **Guo L**, **et al**. The role of histone deacetylase 4 during chondrocyte hypertrophy and endochondral bone development. *Bone Joint Res*. 2020;9(2):82–89.
8. **Bradley EW**, **Carpio LR**, **van Wijnen AJ**, **McGee-Lawrence ME**, **Westendorf JJ**. Histone deacetylases in bone development and skeletal disorders. *Physiol Rev*. 2015;95(4):1359–1381.
9. **Cao K**, **Wei L**, **Zhang Z**, **et al**. Decreased histone deacetylase 4 is associated with human osteoarthritis cartilage degeneration by releasing histone deacetylase 4 inhibition of runt-related transcription factor-2 and increasing osteoarthritis-related genes: a novel mechanism of human osteoarthritis cartilage degeneration. *Arthritis Res Ther*. 2014;16(6):491.
10. **Guan Y**, **Chen Q**, **Yang X**, **et al**. Subcellular relocation of histone deacetylase 4 regulates growth plate chondrocyte differentiation through Ca2+/calmodulin-dependent kinase IV. *Am J Physiol Cell Physiol*. 2012;303(1):C33–40.
11. **Gao L**, **Li S**, **Wei X**, **Du G**, **Wei D**, **Wei L**. Conditional deletion of HDAC4 from collagen type 2α1-expressing cells increases angiogenesis in vivo. *Mol Med*. 2020;26(1):36.
12. **Guo L**, **Wei X**, **Zhang Z**, **et al**. Ipriflavone attenuates the degeneration of cartilage by blocking the Indian hedgehog pathway. *Arthritis Res Ther*. 2019;21(1):109.
13. **Wei L**, **Sun X**, **Kanbe K**, **et al**. Chondrocyte death induced by pathological concentration of chemokine stromal cell-derived factor-1. *J Rheumatol*. 2006;33(9):1818–1826.
14. **Wei L**, **Sun X**, **Wang Z**, **Chen Q**. CD95-induced osteoarthritic chondrocyte apoptosis and necrosis: dependency on p38 mitogen-activated protein kinase. *Arthritis Res Ther*. 2006;8(2):R37.
15. **Fei J**, **Liang B**, **Jiang C**, **Ni H**, **Wang L**. Luteolin inhibits IL-1β-induced inflammation in rat chondrocytes and attenuates osteoarthritis progression in a rat model. *Biomed Pharmacother*. 2019;109:1586–1592.
16. **Bunpetch V**, **Zhang X**, **Li T**, **et al**. Silicate-based bioceramic scaffolds for dual-lineage regeneration of osteochondral defect. *Biomaterials*. 2019;192:323–333.
17. **No authors listed**. MSigDB: Molecular Signatures Database. Gene Set Enrichment Analysis (GSEA). 2023. https://www.gsea-msigdb.org/gsea/msigdb (date last accessed 27 June 2023).
18. **Jay GD**, **Fleming BC**, **Watkins BA**, **et al**. Prevention of cartilage degeneration and restoration of chondroprotection by lubricin tribosupplementation in the rat following anterior cruciate ligament transection. *Arthritis Rheum*. 2010;62(8):2382–2391.
19. **Parra M**, **Verdin E**. Regulatory signal transduction pathways for class IIa histone deacetylases. *Curr Opin Pharmacol*. 2010;10(4):454–460.
20. **Wang AH**, **Kruhlak MJ**, **Wu J**, **et al**. Regulation of histone deacetylase 4 by binding of 14-3-3 proteins. *Mol Cell Biol*. 2000;20(18):6904–6912.
21. **Grozinger CM**, **Schreiber SL**. Regulation of histone deacetylase 4 and 5 and transcriptional activity by 14-3-3-dependent cellular localization. *Proc Natl Acad Sci U S A*. 2000;97(14):7835–7840.
22. **Liu F**, **Dowling M**, **Yang X-J**, **Kao GD**. Caspase-mediated specific cleavage of human histone deacetylase 4. J Biol Chem. 2004;279(33):34537–34546.
23. **Cohen TJ**, **Choi M-C**, **Kapur M**, **Lira VA**, **Yan Z**, **Yao T-P**. HDAC4 regulates muscle fiber type-specific gene expression programs. *Mol Cells*. 2015;38(4):343–348.
24. **Mielcarek M**, **Zielonka D**, **Carnemolla A**, **Marcinkowski JT**, **Guidez F**. HDAC4 as a potential therapeutic target in neurodegenerative diseases: a summary of recent achievements. *Front Cell Neurosci*. 2015;9:42.
25. **Zhang LX**, **Du J**, **Zhao YT**, **et al**. Transgenic overexpression of active HDAC4 in the heart attenuates cardiac function and exacerbates remodeling in infarcted myocardium. *J Appl Physiol (1985)*. 2018;125(6):1968–1978.
26. **Yang D**, **Xiao C**, **Long F**, **et al**. HDAC4 regulates vascular inflammation via activation of autophagy. *Cardiovasc Res*. 2018;114(7):1016–1028.
27. **Barbier-Torres L**, **Beraza N**, **Fernández-Tussy P**, **et al**. Histone deacetylase 4 promotes cholestatic liver injury in the absence of prohibitin-1. *Hepatology*. 2015;62(4):1237–1248.
28. **Wang P**, **Mao Z**, **Pan Q**, **et al**. Histone deacetylase-4 and histone deacetylase-8 regulate interleukin-1β-induced cartilage catabolic degradation through MAPK/JNK and ERK pathways. *Int J Mol Med*. 2018;41(4):2117–2127.

29. **Hou F**, **Wei W**, **Qin X**, **et al**. The posttranslational modification of HDAC4 in cell biology: Mechanisms and potential targets. *J Cell Biochem*. 2020;121(2):930–937.
30. **Zhou X**, **Liao W-J**, **Liao J-M**, **Liao P**, **Lu H**. Ribosomal proteins: functions beyond the ribosome. *J Mol Cell Biol*. 2015;7(2):92–104.
31. **Istiaq A**, **Ohta K**. Ribosome-induced cellular multipotency, an emerging avenue in cell fate reversal. *Cells*. 2021;10(9):2276.
32. **Kappeler KV**, **Zhang J**, **Dinh TN**, **Strom JG**, **Chen QM**. Histone deacetylase 6 associates with ribosomes and regulates de novo protein translation during arsenite stress. *Toxicol Sci*. 2012;127(1):246–255.
33. **Xu Q**, **Liu Q**, **Chen Z**, **et al**. Histone deacetylases control lysine acetylation of ribosomal proteins in rice. *Nucleic Acids Res*. 2021;49(8):4613–4628.
34. **Ficner R**. Novel structural insights into class I and II histone deacetylases. *Curr Top Med Chem*. 2009;9(3):235–240.

Author information:
- L. Guo, PhD, Laboratory Technician
- H. Guo, BD, MD student
- Y. Zhang, BD, MD student
- Z. Chen, MD, Orthopedist
- J. Sun, PhD, Orthopedist
- G. Wu, MD, PhD student
- Y. Wang, MD, PhD student
- Y. Zhang, PhD, Orthopedist
- X. Wei, PhD, Professor
- P. Li, PhD, Professor

Shanxi Key Laboratory of Bone and Soft Tissue Injury Repair, Department of Orthopedics, the Second Hospital of Shanxi Medical University, Taiyuan, China.

Author contributions:
- L. Guo: Conceptualization, Methodology, Investigation, Writing – review & editing.
- H. Guo: Methodology, Formal analysis.
- Y. Zhang: Methodology, Formal analysis.
- Z. Chen: Formal analysis, Writing – review & editing.
- J. Sun: Formal analysis, Writing – review & editing.
- G. Wu: Investigation, Formal analysis.
- Y. Wang: Formal analysis.
- Y. Zhang: Conceptualization, Formal analysis.
- X. Wei: Methodology, Project administration, Writing – original draft.
- P. Li: Conceptualization, Formal analysis, Writing – review & editing.

Funding statement:
- The authors disclose receipt of the following financial or material support for the research, authorship, and/or publication of this article: the project was supported by: National Natural Science Foundation of China (NSFC) grants U21A20353 and 82172503; Natural Science Foundation of Shanxi Province (SXNSF) grants 20210302123285, 20210302123263, 20210302124670, and 20210302123283; and the Doctor Fund of the Second Hospital of Shanxi Medical University, grant 202001-9.

ICMJE COI statement:
- The authors declare that they have no competing interests.

Data sharing:
- All data generated or analyzed during this study are included in the published article and/or in the supplementary material.

Acknowledgements:
- The authors gratefully acknowledge all authors of this article, all funding supporting this project, and Editage (www.editage.cn) for English language editing.

Ethical review statement:
- All animal experiments were approved by the Institutional Review Board (IRB) at the Second Hospital of Shanxi Medical University (Taiyuan, China; CMTT#: 2021012, Approval 2021). Human cartilage samples were obtained from the "relatively normal" cartilage samples of the tibial plateau obtained during total knee arthroplasty. The experiments were approved by the IRB at the Second Hospital of Shanxi Medical University (Taiyuan, China; CMTT#: 2021YX019, Approval 2021).

Open access funding:
- The authors report that they received open access funding for their manuscript from: the National Natural Science Foundation of China (NSFC) grants U21A20353 and 82172503; Natural Science Foundation of Shanxi Province (SXNSF) grants 20210302123285, 20210302123263, 20210302124670, and 20210302123283; and the Doctor Fund of the Second Hospital of Shanxi Medical University, grant 202001-9.